Genetic Alterations That Inhibit In Vivo Pressure-Overload Hypertrophy Prevent Cardiac Dysfunction Despite Increased Wall Stress

Giovanni Esposito, MD; Antonio Rapacciuolo, MD; Sathyamangla V. Naga Prasad, PhD;
Hideyuki Takaoka, MD, PhD; Steven A. Thomas, MD, PhD;
Walter J. Koch, PhD; Howard A. Rockman, MD

Background—A long-standing hypothesis has been that hypertrophy is compensatory and by normalizing wall stress acts to maintain normal cardiac function. Epidemiological data, however, have shown that cardiac hypertrophy is associated with increased mortality, thus casting doubt on the validity of this hypothesis.

Methods and Results—To determine whether cardiac hypertrophy is necessary to preserve cardiac function, we used 2 genetically altered mouse models that have an attenuated hypertrophic response to 8 weeks of pressure overload. End-systolic wall stress (σ_{es}) obtained by sonomicrometry after 1 week of pressure overload showed complete normalization of σ_{es} in pressure-overloaded wild-type mice (287 ± 39 versus sham, 254 ± 34 g/cm^2), whereas the blunted hypertrophic response in the transgenic mice was inadequate to normalize σ_{es} (415 ± 81 g/cm^2, $P<0.05$). Remarkably, despite inadequate normalization of σ_{es}, cardiac function as measured by serial echocardiography showed little deterioration in either of the pressure-overloaded genetic models with blunted hypertrophy. In contrast, wild-type mice with similar pressure overload showed a significant increase in chamber dimensions and progressive deterioration in cardiac function. Analysis of downstream signaling pathways in the late stages of pressure overload suggests that phosphoinositide 3-kinase may play a pivotal role in the transition from hypertrophy to heart failure.

Conclusions—These data suggest that under conditions of pressure overload, the development of cardiac hypertrophy and normalization of wall stress may not be necessary to preserve cardiac function, as previously hypothesized. (***Circulation***. 2002;105:85-92.)

Key Words: contractility ■ hypertrophy ■ heart failure ■ receptors, adrenergic, beta ■ signal transduction

Heart failure is a major health problem estimated to affect 700 000 individuals per year in the United States alone.[1] An important cause of heart failure is chronic pressure overload, such as that which occurs with longstanding hypertension. At a cellular level, myocytes respond to pressure overload with the parallel addition of sarcomeres, resulting in an increase in myocyte width and ventricular wall thickness.[2]

See p 8

It has been a long-standing hypothesis that the development of myocardial hypertrophy is a compensatory mechanism in response to disease states that produce increased cardiac workload to normalize wall stress and maintain normal cardiac function, thereby preventing the development of heart failure.[2,3] Although this remodeling may act to normalize wall stress, results from the Framingham Heart Study show an association between ventricular hypertrophy and increased cardiac mortality,[4] casting doubt on the validity of the wall-stress hypothesis. Thus, whether cardiac hypertrophy in response to pressure overload is adaptive or maladaptive remains a fundamental issue in the pathogenesis of heart failure.

To address this issue, we studied the effect of long-term pressure overload on the development of heart failure using 2 murine models that have an attenuated hypertrophic response to pressure overload: (1) cardiac gene–targeted mice with the myocardial expression of a carboxyl terminal peptide of Gα_q (TgGqI) that specifically inhibits G$_q$-mediated signaling[5] and (2) genetically altered mice that lack endogenous norepinephrine and epinephrine created by disruption of the dopamine β-hydroxylase gene (Dbh$^{-/-}$), the essential enzyme in the biosynthetic pathway converting dopamine to norepinephrine.[6,7]

Circulation is available at http://www.circulationaha.org

Methods

Experimental Animals

Genetically altered and strain-matched wild-type mice 3 to 4 months of age were used for this study.[5–8] Animals were handled according to approved protocols and animal welfare regulations by the Institutional Review Board at Duke University Medical Center.

Transthoracic Echocardiography

2D guided M-mode echocardiography was performed in conscious mice with an HDI 5000 echocardiograph (ATL) as previously described.[9]

In Vivo Pressure Overload

Mice were anesthetized with a mixture of ketamine (100 mg/kg) and xylazine (2.5 mg/kg), and transverse aortic constriction (TAC) was performed as previously described.[10] Eight weeks after surgery, the transstenotic gradient was assessed by recording the simultaneous measurement of right carotid and left axillary arterial pressures.

Pressure-Volume and Stress-Strain Analysis in 7-Day Pressure-Overloaded Mice

In separate experiments 7 days after TAC, pressure-volume and stress-strain analysis was performed as previously described with modifications.[9] After the chest had been opened, afterload was normalized by removal of the 7-day suture, and a new suture ligature was placed around the transverse aorta to manipulate loading conditions. Five miniature piezoelectric crystals (4 endocardial and 1 epicardial) were implanted in the beating heart to obtain 2 orthogonal dimensions and instantaneous wall thickness throughout the cardiac cycle (Sonometrics). The end-systolic pressure, the end-systolic volume, the volume axis intercept, and the slope of the end-systolic pressure-volume relation (E'_{max}) value reflecting cardiac contractility were obtained. Instantaneous stress (σ) and strain (ϵ) were calculated and stress-strain loops generated as described.[11] Maximum systolic stiffness (E_{aVmax}), an index of left ventricular (LV) contractility independent of ventricular size, was obtained from the following relation: $\sigma_{es} = E_{aVmax} \times \epsilon_{es}$, where σ_{es} is end-systolic stress and ϵ_{es} is end-systolic midwall natural strain.

Mitogen-Activated Protein Kinase Activity

Mitogen-activated protein kinase (MAPK) activities were assessed from LV extracts as the capacity of immunoprecipitated ERK2-p42/ERK1-p44, p38, p38β, and JNK1-p46/JNK3 MAPK to phosphorylate in vitro substrates (myelin basic protein or GST-cJun) as described.[12]

G Protein–Coupled Receptor Kinase Activity by Rhodopsin Phosphorylation

Cytosolic extracts (300 μg of protein) were incubated with rhodopsin-enriched rod outer segments in 25 μL of lysis buffer with 10 mmol/L MgCl$_2$ and 0.1 mmol/L ATP containing [γ-^{32}P]ATP.[13] Reactions were incubated in white light for 15 minutes, quenched with 300 μL of ice-cold lysis buffer, centrifuged, and resolved by SDS-PAGE.[13] Phosphorylated rhodopsin was visualized by autoradiography and quantified with a PhosphorImager.

Immunoblotting

Immunodetection of myocardial levels of β-adrenergic receptor kinase 1 (βARK1) was performed on cytosolic extracts with a polyclonal anti-βARK1 antibody (Santa Cruz Biotechnology) as previously described.[13] After transfer to polyvinylidine difluoride membrane (Biorad), the 80-kDa βARK1 protein was visualized by chemiluminescence detection (ECL, Amersham).

βAR Density and Adenylyl Cyclase Activity

Myocardial membranes were prepared by homogenization of whole hearts in ice-cold buffer as described.[13] Total βAR density was determined by incubation of 25 μg of membranes with a saturating concentration (80 pmol/L) of ^{125}I-labeled cyanopindolol and 20 mmol/L alprenolol to define nonspecific binding.[13,14] Assays were conducted at 37°C for 60 minutes and then filtered over GF/C glass fiber filters (Whatman), then washed and counted in a gamma counter. Adenylyl cyclase activity was measured as described[15] on purified cardiac membranes.

Phosphoinositide 3-Kinase and v-Akt Activity

Phosphoinositide 3-kinase (PI3K) activity was performed on clarified myocardial extracts after immunoprecipitation with an antibody to PI3K as previously described.[16,17] Phosphorylated active v-Akt from cardiac extracts prepared as above was detected by immunoblotting with rabbit polyclonal phospho-Akt (Ser473) and rabbit polyclonal Akt (Ser473) antibodies (Cell Signaling Technology).[16]

Statistical Analysis

Data are expressed as mean±SEM. Two-way repeated-measures ANOVA was used to evaluate the echo measurements, end-systolic pressure-volume relation, and stress-strain variables under basal conditions and with dobutamine stimulation. When appropriate, post hoc analysis was performed with a Scheffé test. For all analyses, a value of $P < 0.05$ was considered significant. For the data from MAPK signaling, 2-sample comparisons were performed with Student's t test, and multigroup comparisons were made with a 1-way ANOVA and Tukey's test.
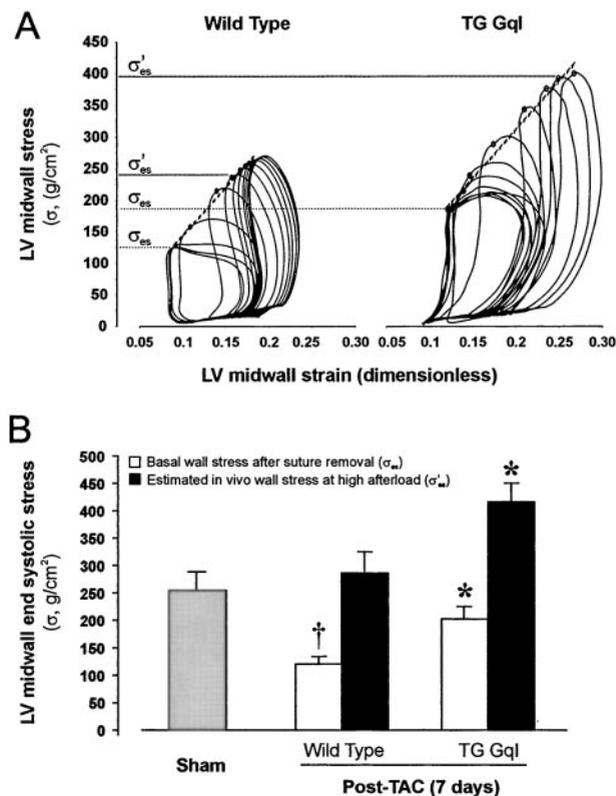

Figure 1. In vivo stress-strain relations in pressure-overloaded wild-type and TgGqI mouse hearts. A, Representative stress-strain tracings 7 days after TAC. B, Basal σ_{es} and estimated in vivo wall stress (σ'_{es}) at high afterload in sham wild-type (n=5), TAC wild-type (n=5), and TAC TgGqI (n=5) mice. Systolic wall stress was normalized only in wild-type TAC hearts. †$P < 0.02$ vs sham; *$P < 0.02$ basal TgGqI vs sham, and TgGqI at high afterload vs wild-type at high afterload.

Results

Wall Stress and Stress-Strain Relations in 7-Day Banded Mice

In vivo wall stress in banded wild-type and TgGqI mice was measured 7 days after TAC (Figure 1). End-systolic wall stress (σ_{es}) in pressure-overloaded hearts was calculated from the stress-strain loops after removal of the suture surrounding the transverse aorta. To estimate the in vivo end-systolic wall stress (σ'_{es}) in the intact-banded mouse heart, the pressure gradient before removal of the suture was added to the LV systolic pressure measured after removal of the suture. Wall stress was completely normalized in banded wild-type mice because of the induction of adequate hypertrophy (Figure 1, A and B; Table 1). In contrast, wall stress was significantly elevated in banded TgGqI mice because the level of hypertrophy was inadequate (Figure 1, A and B, Table 1). Furthermore, basal and agonist-stimulated contractile function, measured by LV dP/dt$_{max}$ and E'$_{max}$, were similar in banded wild-type and TgGqI mice (Table 1).

Physiological Response to Long-Term In Vivo Pressure Overload in Wild-Type and TgGqI Mice

Serial echocardiography was performed in conscious wild-type and TgGqI mice before and 4 weeks and 8 weeks after TAC. Wild-type mice developed progressive LV enlargement and dysfunction, as shown by a 40% reduction in percent fractional shortening (%FS), a 100% increase in LV end-systolic dimension (LVESD), and a 27% increase in LV end-diastolic dimension (LVEDD) compared with the basal measurements (Figure 2, A through D, Table 2). In contrast, the TgGqI mice showed significantly less deterioration in cardiac function than the wild-type banded mice (Figure 2, A through D, Table 2).

At 8 weeks after TAC, the increase in the ratio of LV weight to body weight (LVW/BW) in banded TgGqI mice was significantly blunted compared with the banded wild-type mice, despite a similar transstenotic pressure gradient (Figure 2E, Table 2). Postsurgical mortality in banded TgGqI mice was not different from that in wild-type mice at 16% and 18%, respectively. In addition, peak LV systolic pressure, as measured by the carotid arterial pressure proximal to the stenosis, was not different after TAC in the TgGqI mice from that in control mice (190.2±6.2 versus 183.1±8.3 mm Hg), confirming matched hemodynamic loads.

Physiological Response to Long-Term In Vivo Pressure Overload in *Dbh*$^{-/-}$ and Control Mice

TAC in control mice resulted in a significant reduction in %FS and an increase in LVESD and LVEDD compared with baseline measurements (Figure 3, A through D, Table 3). In marked contrast, LVESD, LVEDD, and %FS in *Dbh*$^{-/-}$ mice remained essentially normal 4 and 8 weeks after TAC compared with the pre-TAC measurements (Figure 3, A through D, Table 3). Remarkably, even though cardiac hypertrophy in *Dbh*$^{-/-}$ mice was significantly inhibited (Figure 3, E and F, Table 3), there was no deterioration of cardiac function. Postsurgical mortality in banded *Dbh*$^{-/-}$ mice was not different from that in wild-type mice at 17% and 21%,

TABLE 1. Invasive Hemodynamics in 7-Day Banded Wild-Type and TgGqI Mice

	Wild-Type (n=5)		TgGqI (n=5)	
	Basal	Dobutamine	Basal	Dobutamine
HR, bpm	289±9	371±4	330±41	378±21
LVESP, mm Hg	79±4	90±3	88±18	105±10
LVEDP, mm Hg	11.6±1.5	7.8±1.6	9.5±2.0	10.3±1.1
TSPG, mm Hg	77±5		67±9	
V$_{ed}$, μL	46±7	43±5	30±2	31±1
V$_{es}$, μL	36±6	35±4	25±2	25±1
LV dP/dt$_{max}$, mm Hg/s	3714±369	5237±150‡	5034±1265	8959±728‡
E'$_{max}$, mm Hg/μL	23.2±3.3	36.7±4.1§	33.0±15.3	56.2±7.9§
V$_0$, μL	34±7	34±5	23±2	23±1
r^2	0.995±0.002	0.999±0.001	0.994±0.006	0.983±0.003
Systolic myocardial stiffness	2562±626	2771±268	3138±1321	5468±568
σ_{es}, g/cm^2	121±14	156±15	202±49*	218±27
σ'_{es}, g/cm^2	287±39	326±20	415±81†	420±49
BW, g	26.1±1.8		23.0±4.6	
LVW/BW, mg/g	5.44±0.32		4.31±0.44*	

HR indicates heart rate; LVESP, LV end-systolic pressure; LVEDP, LV end-diastolic pressure; TSPG, transstenotic systolic pressure gradient as the difference between right and left carotid and left axillary artery systolic pressures; V$_{ed}$, LV end-diastolic volume; V$_{es}$, LV end-systolic volume; LV dP/dt$_{max}$, maximal first derivative of LV pressure; E'$_{max}$, local slope at V$_0$; V$_0$, volume axis intercept; σ_{es}, basal end-systolic wall stress after TAC removal; σ'_{es}, estimated end-systolic in vivo wall stress at high afterload; BW, body weight; and LVW/BW, LV weight–to–body weight ratio calculated using the maximal body weight from either before or after TAC.

*$P<0.02$, †$P<0.05$ vs wild-type basal; ‡$P<0.02$, §$P<0.05$ vs wild-type basal or TgGqI basal.

TABLE 2.   Echocardiography in Wild-Type and TgGqI Mice Before and After TAC

	Wild-Type (n=22)			TgGqI (n=15)		
		After			After	
	Before	4 Weeks	8 Weeks	Before	4 Weeks	8 Weeks
LVEDD, mm	3.1±0.1	3.4±0.1	3.9±0.1‡	3.1±0.1	3.2±0.1	3.4±0.2†
LVESD, mm	1.3±0.1	1.9±0.1‡	2.6±0.2‡	1.2±0.1	1.5±0.2	1.7±0.2*
%FS	59±0.8	44±2.3‡	35±2.6‡	60±1.0	56±3.0†	52±4.0*‡
SEPth, mm	0.6±0.1	0.9±0.1‡	1.0±0.1‡	0.6±0.1	0.7±0.1	0.9±0.1‡
PWth, mm	0.5±0.1	0.7±0.1‡	0.8±0.1‡	0.5±0.1	0.6±0.1	0.8±0.1‡
HR, bpm	621±9	612±12	612±10	611±11	623±15	610±10
Mean Vcfc, circ/s	4.05±0.1	3.07±0.1	2.35±0.2‡	4.3±0.1	4.2±1.5	4.0±0.4†
BW, g	23.8±0.6		26.4±0.7‡	22.4±1.1		26.1±0.9‡
LVW/BW, mg/g			6.28±0.27			5.2±0.3†
TSPG, mm Hg			82.0±4.3			76.5±6.4

%FS was calculated as (LVEDD−LVESD)/LVEDD. SEPth indicates septal wall thickness; PWth, posterior wall thickness; mean Vcfc, heart rate–corrected mean velocity of circumferential fiber shortening calculated as FS divided by ejection time multiplied by the square root of the R-R interval. Other abbreviations as in Table 1.

*$P<0.001$, †$P<0.01$, TgGqI vs wild-type at same time point; ‡$P<0.01$ vs before TAC in same group.

respectively. In addition, peak LV systolic pressure was not different after TAC in the $Dbh^{-/-}$ mice compared with control mice (178.5±6.4 versus 174.1±5.5 mm Hg). These data show that the blunting of the hypertrophic response and the resultant increase in wall stress are associated with less deterioration in cardiac function despite the continued presence of a pressure load on the heart.

βAR Signaling in Banded TgGqI and $Dbh^{-/-}$ Mice

βAR levels, adenylyl cyclase activity, and βARK1 activity were measured in hearts from TgGqI and $Dbh^{-/-}$ mice after 8 weeks of pressure overload. βAR downregulation occurred after TAC in both wild-type and TgGqI mice but was prevented in the $Dbh^{-/-}$ mice (Figure 4, A and D).

Furthermore, the impaired adenylyl cyclase activity observed in the wild-type banded mice (Figure 4, B and E) was not observed in either the banded TgGqI or $Dbh^{-/-}$ mice (Figure 4, B and E). NaF-stimulated adenylyl cyclase activity was impaired only in wild-type banded hearts, indicating a significant defect in postreceptor signaling (data not shown). Finally, a significant increase in G protein–coupled receptor kinase activity was detected in both wild-type and TgGqI banded hearts but was unchanged in the banded $Dbh^{-/-}$ mice (Figure 4, C and F). Taken together, these data suggest that the greater the attenuation of the hypertrophic response with chronic pressure overload, the less development of heart failure and the fewer abnormalities in βAR signaling.
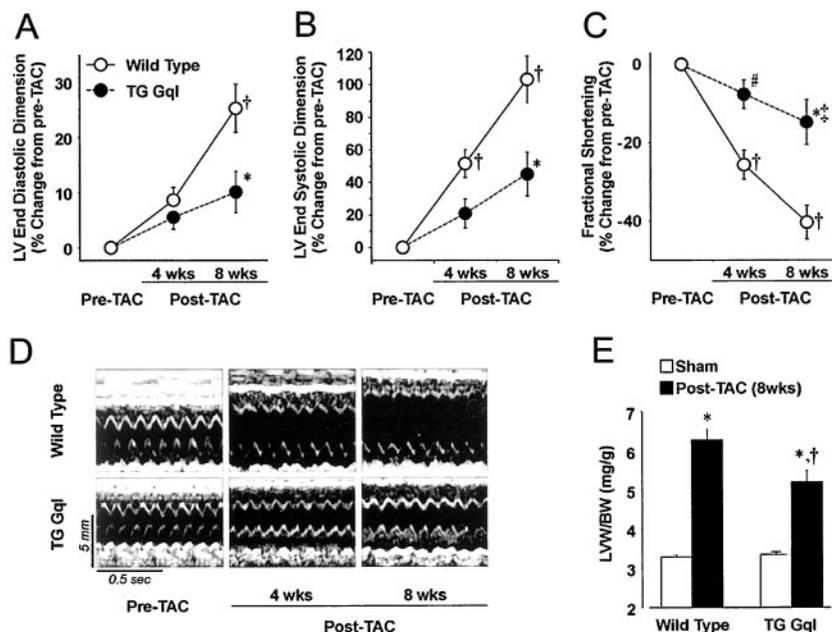

Figure 2. Serial echocardiography in conscious wild-type and TgGqI mice with chronic pressure overload. A, LVEDD; B, LVESD; and C, FS. *$P<0.005$, #$P<0.05$, TgGqI vs wild-type at same time after TAC; †$P<0.001$ wild-type TAC vs before TAC; ‡$P<0.05$ TgGqI at 8 weeks vs before TAC. D, Representative serial M-mode echocardiographic tracings before and 4 weeks and 8 weeks after TAC. E, LVW/BW in banded wild-type and TgGqI mice 8 weeks after TAC. *$P<0.01$ TAC vs sham either wild-type or TgGqI; †$P<0.01$ TAC TgGqI vs TAC wild-type.
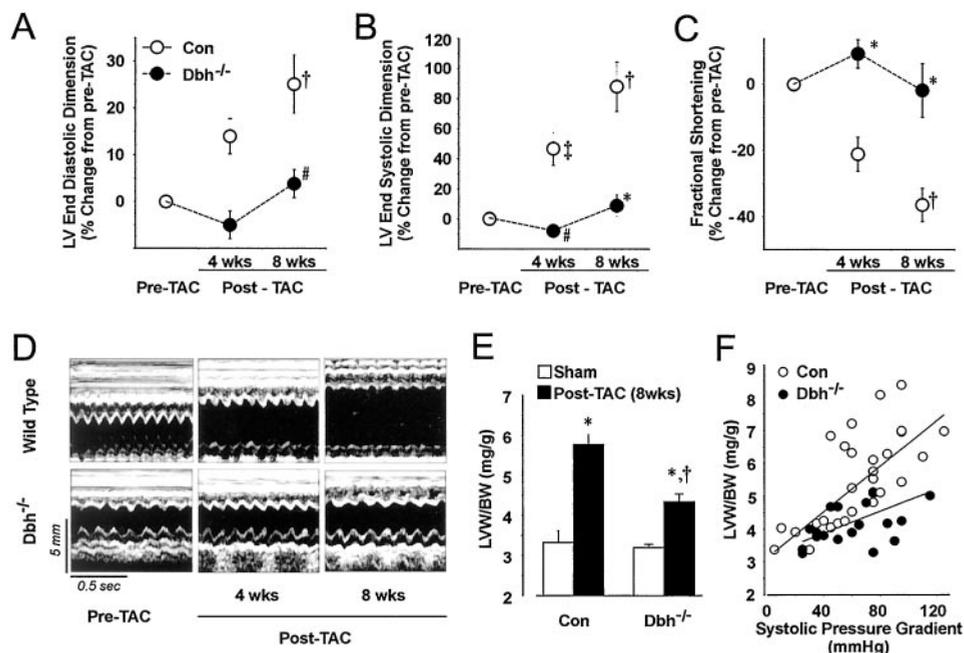
Figure 3. Serial echocardiography in conscious control and *Dbh*⁻/⁻ mice with chronic pressure overload. A, LVEDD; B, LVESD; C, FS. *P<0.005, #P<0.05, *Dbh*⁻/⁻ vs control at same time after TAC; †P<0.001, ‡P<0.05 control TAC vs before TAC. D, Representative serial M-mode echocardiographic tracings before and 4 weeks and 8 weeks after TAC. E and F, LVW/BW in control and *Dbh*⁻/⁻ mice 8 weeks after TAC. *P<0.01 TAC *Dbh*⁻/⁻ or control vs sham; †P<0.01 TAC *Dbh*⁻/⁻ vs TAC control.

MAPK Signaling in Heart Failure

Because recent studies have shown that internalization of βARs can lead to activation of MAPK signaling pathways,[18,19] we evaluated ERK1/2, JNK, p38, and p38β activity in heart extracts 8 weeks after TAC. All 3 MAPK pathways were activated in wild-type TAC hearts at 8 weeks (Figure 5, A and B). Importantly, ERK activation was significantly attenuated in hearts from banded TgGqI and *Dbh*⁻/⁻ mice (Figure 5, A and B).

PI3K and v-Akt in Long-Term Pressure Overload

We recently showed that short-term pressure overload activates PI3K signaling,[16] and this may contribute to internal-

ization of βARs.[17] To determine whether PI3K signaling was altered after chronic pressure overload, we measured PI3K activity in sham and TAC hearts. Whereas PI3K and v-Akt were significantly activated in wild-type banded hearts (Figure 5, C and D), no increase in the PI3K pathway was observed in either the banded TgGqI mice or *Dbh*⁻/⁻ mice (Figure 5, C and D).

Discussion

In this study, we demonstrate that in the mouse, the development of pressure-overload cardiac hypertrophy and normalization of wall stress does not prevent LV decompensa-

TABLE 3. Echocardiography in Control and *Dbh*⁻/⁻ Mice Before and After TAC

	Controls (n=28)			*Dbh*⁻/⁻ (n=18)		
		After			After	
	Before	4 Weeks	8 Weeks	Before	4 Weeks	8 Weeks
LVEDD, mm	3.5±0.1	4.0±0.2	4.4±0.3‡	3.6±0.1	3.4±0.1	3.7±0.2†
LVESD, mm	1.5±0.1	2.3±0.3	3.0±0.4‡	2.2±0.1	2.0±0.1	2.4±0.2
%FS	56±1.4	44±4.2	36±4.0‡	38±1.3*	41±1.4	37±3.1
SEPth, mm	0.8±0.1	1.2±0.1‡	1.2±0.1‡	0.7±0.1	0.8±0.1†	0.8±0.1†
PWth, mm	0.7±0.1	0.8±0.1	0.8±0.1	0.6±0.1	0.7±0.1	0.6±0.1*
HR, bpm	631±18	625±14	575±15	443±13*	496±11*	435±14*
Mean Vcfc, circ/s	3.5±0.1	2.8±0.2	2.6±0.3	2.4±0.1	2.6±0.1	2.2±0.2
BW, g	32.7±1.0		33.2±0.9	25.3±0.7†		26.3±0.6†
LVW/BW, mg/g			5.8±0.3			4.3±0.2†
TSPG, mm Hg			69±4			67±5

Abbreviations as in Table 2.

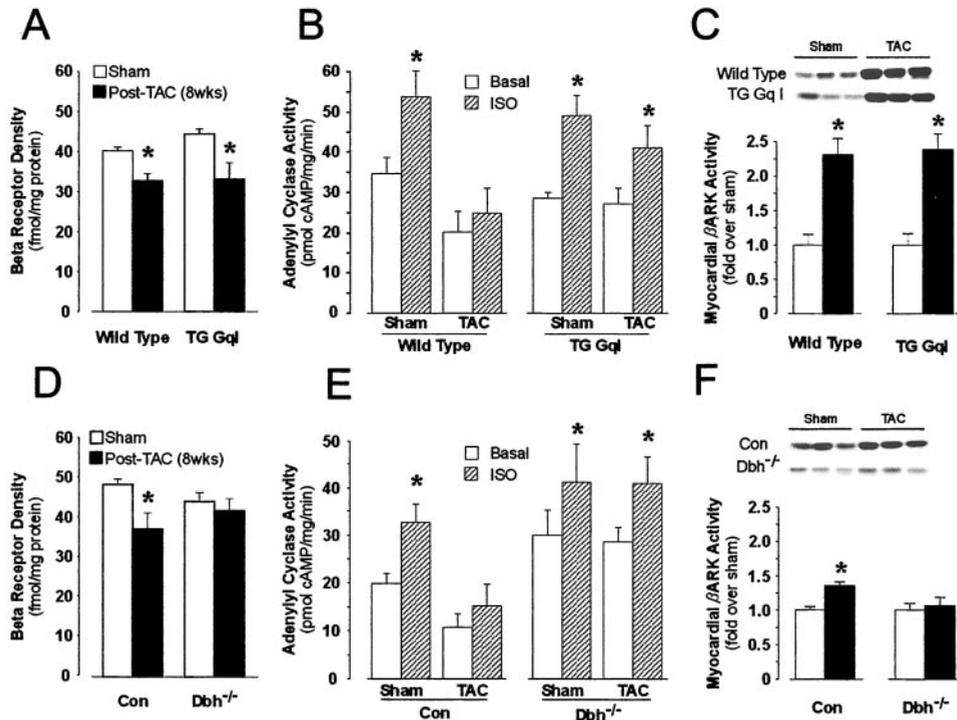*P<0.001, †P<0.01 *Dbh*⁻/⁻ vs wild-type at same time point; ‡P<0.01 vs before TAC in same group.

Figure 4. βAR signaling in TgGqI and *Dbh*^{−/−} mice. βAR density, adenylyl cyclase activity, and myocardial βARK1 activity in TgGqI (A, B, and C) and *Dbh*^{−/−} (D, E, and F) hearts. ISO indicates isoproterenol; Con, control. *$P<0.01$ either TAC vs sham or ISO vs basal, n=5 for each group.

tion, as was previously hypothesized,[2,3] but in fact is associated with progressive deterioration in cardiac function and LV chamber enlargement. Strikingly, in 2 different models, limiting the development of hypertrophy in response to chronic pressure overload is associated with little or no deterioration in cardiac function. By sonomicrometry, we show that normalization of wall stress did indeed occur in hypertrophied wild-type mice, whereas wall stress was increased by 2-fold in the TgGqI mice because of the lack of adequate hypertrophy. Thus, even though wall stress was not normalized in the TgGqI mice, these animals had significantly less LV deterioration with chronic pressure overload, demonstrating that elevated wall stress per se is not a trigger for ventricular decompensation.

PI3Ks are a conserved family of lipid kinases that play a pivotal role in cell proliferation, differentiation, cytoskeletal organization, membrane trafficking, and apoptosis.[20] The finding of total ablation of PI3K activation in pressure-overloaded TgGqI and *Dbh*^{−/−} mice compared with their banded wild-type controls may provide insight into the mechanisms involved. First, lack of PI3K activation can be observed with short-term (7-day) banding in TgGqI mice,[16] a time point before the deterioration in LV function in wild-type banded mice. Second, ERK activation can occur via a PI3K-dependent pathway,[21] which may account, in part, for the inhibition of ERK activation seen in both TgGqI and *Dbh*^{−/−} mice after long-term TAC. Finally, human heart failure is associated with downregulation and desensitization of βARs,[22] and recent studies have shown a pivotal role for PI3K in the process of βAR sequestration.[17] In this study,

pressure-overloaded *Dbh*^{−/−} and TgGqI mice have little or mild alteration in cardiac βAR signaling at 8 weeks, a time when banded control mice have impaired βAR signaling. Taken together, the absence of PI3K activation in the TgGqI and *Dbh*^{−/−} hearts after TAC suggests an important role for PI3K signaling in preventing heart failure progression after pressure overload that may be mediated through its effects on βAR signaling.

Perhaps the signaling cascade most involved in the myocardial hypertrophic response is the MAPKs, including the ERK, JNK, and p38 kinases.[23] All MAPKs were significantly activated 8 weeks after TAC in wild-type control mice, similar to what has been reported in human heart failure.[24] In contrast, ERK was not activated in the TgGqI and *Dbh*^{−/−} animals after TAC and may be a potential mechanism for the lack of deterioration in cardiac function. It has been postulated that in the hypertrophied heart, a chronic reduction in the ability to oxidize fats, resulting primarily from an ERK-mediated reduction in peroxisome proliferator–activated receptor-α activity, may be maladaptive.[25] Furthermore, recent evidence has linked agonist-induced internalization of βARs to activation of the ERK pathway.[18,19] Taken together, we postulate that if the activation of PI3K is blocked during the development of cardiac hypertrophy, the efficiency of βAR internalization is diminished, leading to less ERK activation and a more favorable metabolic state in which fatty acids are used instead of glucose as the primary energy source.

Our study is consistent with recent reports showing no difference in cardiac function between hypertrophic and
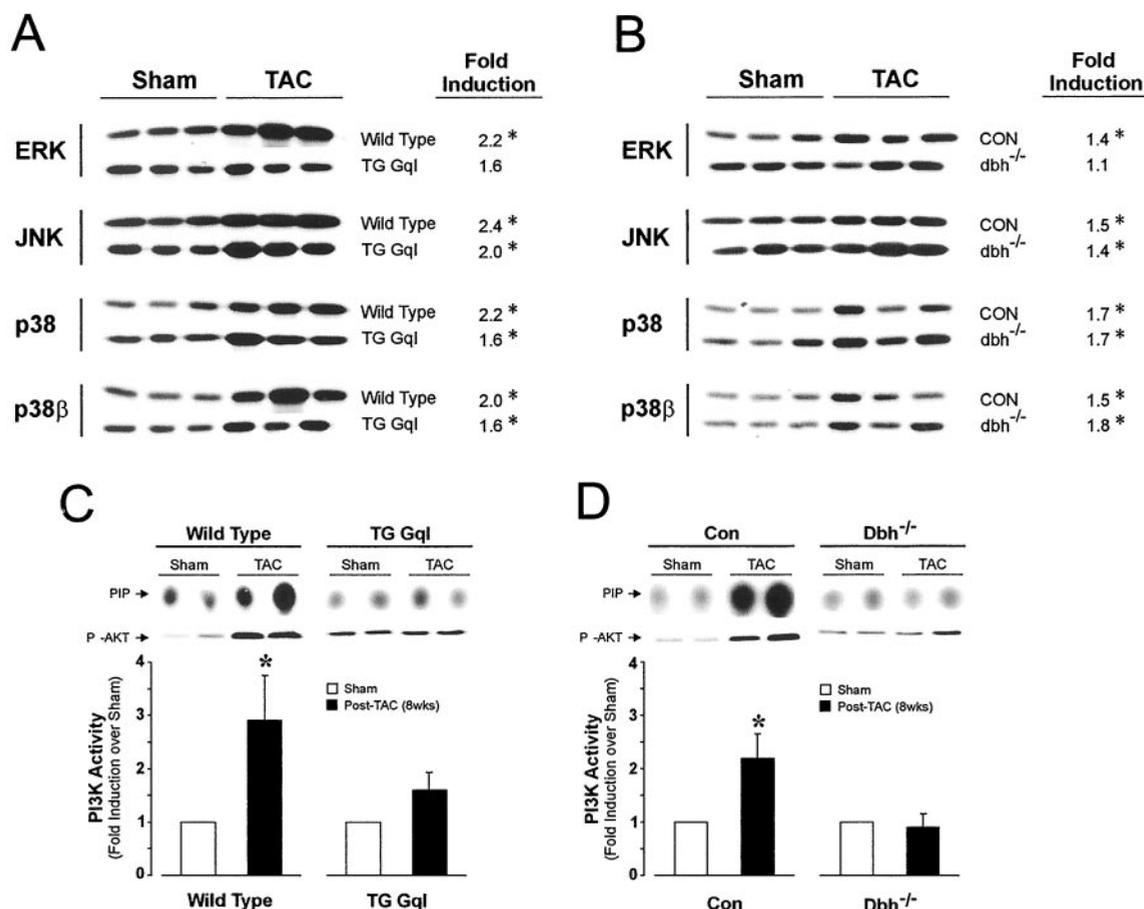
Figure 5. MAPK, PI3K, and v-AKT activity in TgGqI and *Dbh*$^{-/-}$ mice. ERK, JNK, p38, and p38β MAPK activities in LV extracts from 8-week-banded (A) TgGqI and (B) *Dbh*$^{-/-}$ hearts. Numbers represent fold induction, n=8 each group, *P<0.01 TAC vs sham. Total PI3K activity in heart extracts from (C) wild-type and TgGqI mice and (D) control and *Dbh*$^{-/-}$ mice. Top, Phosphorylation of PtdIns to PtdIns(3)P (PIP). Middle, Immunoblot of phospho-AKT. Bottom, Average PI3K activity in sham-operated and TAC hearts (n=8 each group). *P<0.01 TAC vs sham.

nonhypertrophic pressure-overloaded hearts in mice by either treatment with cyclosporine[26] or deletion of the fibroblast growth factor-2 gene.[27] Both studies were limited, however, because neither of the control study groups developed cardiac dysfunction over the time period examined.[26,27]

In conclusion, our study suggests that the development of cardiac hypertrophy and normalization of wall stress are not necessary to preserve cardiac function and that inhibition of PI3K may play an important role in the transition from hypertrophy to failure. These findings may have several important clinical implications in developing new therapeutic strategies to prevent the transition from cardiac hypertrophy to heart failure.

References

1. Abraham WT, Bristow MR. Specialized centers for heart failure management. *Circulation*. 1997;96:2755–2757.
2. Grossman W, Jones D, McLaurin LP. Wall stress and patterns of hypertrophy in the human left ventricle. *J Clin Invest*. 1975;56:56–64.
3. Chien KR. Genomic circuits and the integrative biology of cardiac diseases. *Nature*. 2000;407:227–232.
4. Levy D, Garrison RJ, Savage DD, et al. Prognostic implications of echocardiographically determined left ventricular mass in the Framingham Heart Study. *N Engl J Med*. 1990;322:1561–1566.
5. Akhter SA, Luttrell LM, Rockman HA, et al. Targeting the receptor-Gq interface to inhibit in vivo pressure overload myocardial hypertrophy. *Science*. 1998;280:574–577.
6. Thomas SA, Matsumoto AM, Palmiter RD. Noradrenaline is essential for mouse fetal development. *Nature*. 1995;374:643–646.
7. Cho MC, Rao M, Koch WJ, et al. Enhanced contractility and decreased β-adrenergic receptor kinase-1 in mice lacking endogenous norepinephrine and epinephrine. *Circulation*. 1999;99:2702–2707.
8. Rapacciuolo A, Esposito G, Caron K, et al. Important role of endogenous norepinephrine and epinephrine in the development of in vivo pressure-overload cardiac hypertrophy. *J Am Coll Cardiol*. 2001;38:876–882.
9. Esposito G, Santana LF, Dilly K, et al. Cellular and functional defects in a mouse model of heart failure. *Am J Physiol*. 2000;279:H3101–H3112.
10. Rockman HA, Ross RS, Harris AN, et al. Segregation of atrial-specific and inducible expression of an atrial natriuretic factor transgene in an in vivo murine model of cardiac hypertrophy. *Proc Natl Acad Sci U S A*. 1991;88:8277–8281.

11. Mirsky I, Tajimi T, Peterson KL. The development of the entire end-systolic pressure-volume and ejection fraction-afterload relations: a new concept of systolic myocardial stiffness. *Circulation*. 1987;76: 343–356.

12. Esposito G, Prasad SV, Rapacciuolo A, et al. Cardiac overexpression of a G_q inhibitor blocks induction of extracellular signal–regulated kinase and c-Jun NH_2-terminal kinase activity in in vivo pressure overload. *Circulation*. 2001;103:1453–1458.

13. Choi DJ, Koch WJ, Hunter JJ, et al. Mechanism of beta-adrenergic receptor desensitization in cardiac hypertrophy is increased beta-adrenergic receptor kinase. *J Biol Chem*. 1997;272:17223–17229.

14. Rockman HA, Chien KR, Choi DJ, et al. Expression of a beta-adrenergic receptor kinase 1 inhibitor prevents the development of myocardial failure in gene-targeted mice. *Proc Natl Acad Sci U S A*. 1998;95: 7000–7005.

15. Harding V, Jones L, Lefkowitz R, et al. Cardiac βARK inhibition improves survival and augments β blocker therapy in a mouse model of severe heart failure. *Proc Natl Acad Sci U S A*. 2001;98:5809–5814.

16. Naga Prasad SV, Esposito G, Mao L, et al. $G\beta\gamma$-dependent phosphoinositide 3-kinase activation in hearts with in vivo pressure overload hypertrophy. *J Biol Chem*. 2000;275:4693–4698.

17. Naga Prasad SV, Barak LS, Rapacciuolo A, et al. Agonist-dependent recruitment of phosphoinositide 3-kinase to the membrane by β-adrenergic receptor kinase 1: a role in receptor sequestration. *J Biol Chem*. 2001;276:18953–18959.

18. Daaka Y, Luttrell LM, Ahn S, et al. Essential role for G protein-coupled receptor endocytosis in the activation of mitogen-activated protein kinase. *J Biol Chem*. 1998;273:685–688.

19. Luttrell LM, Ferguson SS, Daaka Y, et al. Beta-arrestin-dependent formation of beta2 adrenergic receptor-Src protein kinase complexes. *Science*. 1999;283:655–661.

20. Rameh LE, Cantley LC. The role of phosphoinositide 3-kinase lipid products in cell function. *J Biol Chem*. 1999;274:8347–8350.

21. Lopez-Ilasaca M, Crespo P, Pellici PG, et al. Linkage of G protein-coupled receptors to the MAPK signaling pathway through PI 3-kinase gamma. *Science*. 1997;275:394–397.

22. Bristow MR. Why does the myocardium fail? Insights from basic science. *Lancet*. 1998;352(suppl 1):SI8–SI14.

23. Sugden PH. Signaling in myocardial hypertrophy: life after calcineurin? *Circ Res*. 1999;84:633–646.

24. Haq S, Choukroun G, Lim H, et al. Differential activation of signal transduction pathways in human hearts with hypertrophy versus advanced heart failure. *Circulation*. 2001;103:670–677.

25. Barger PM, Brandt JM, Leone TC, et al. Deactivation of peroxisome proliferator-activated receptor-alpha during cardiac hypertrophic growth. *J Clin Invest*. 2000;105:1723–1730.

26. Hill JA, Karimi M, Kutschke W, et al. Cardiac hypertrophy is not a required compensatory response to short-term pressure overload. *Circulation*. 2000;101:2863–2869.

27. Schultz JE, Witt SA, Nieman ML, et al. Fibroblast growth factor-2 mediates pressure-induced hypertrophic response. *J Clin Invest*. 1999; 104:709–719.

Circulation

American Heart Association®

Genetic Alterations That Inhibit In Vivo Pressure-Overload Hypertrophy Prevent Cardiac Dysfunction Despite Increased Wall Stress

Giovanni Esposito, Antonio Rapacciuolo, Sathyamangla V. Naga Prasad, Hideyuki Takaoka, Steven A. Thomas, Walter J. Koch and Howard A. Rockman

The online version of this article, along with updated information and services, is located on the World Wide Web at:

http://circ.ahajournals.org/content/105/1/85